A MICROCONTROLLER BASED 100 kHz - 1 MHz MULTI-FREQUENCY BIO-IMPEDANCE MEASUREMENT DEVICE

by

Hakan Solmaz

B.S. in Physics, Boğaziçi University, 2005

Submitted to the Institute of Biomedical Engineering
in partial fulfillment of the requirements
for the degree of
Master of Science
in
Biomedical Science

Boğaziçi University
June 2008

ACKNOWLEDGMENTS

I would like to express my special thanks to my thesis advisor, Prof. Dr. Yekta Ülgen, for his guidance and valuable criticism throughout my study.

I am very thankful to Murat Tümer for his continuous help and patience during this study.

I would like to thank Deniz Nevşehirli for supporting me at any step of my thesis.

I am very thankful to Ömer Şayli for his continuous help during my study.

I would like to thank my family for their support and belief for my thesis.

I am very specially thankful to my wife Edona Solmaz for her support and encouragement during my work.

ABSTRACT

A MICROCONTROLLER BASED 100 kHz - 1 MHz MULTI-FREQUENCY BIO-IMPEDANCE MEASUREMENT DEVICE

Complex impedance measurement of biological systems is gaining wide popularity in determining the pathological and physiological status of biological tissues in research applications such as; skin hydration, dental decay, body fat content, tissue ischemia, food freshness, blood freshness and etc.

The device presented in this study is a four-probe, multi frequency, portable bio-impedance measurement device based on the principles of magnitude-ratio and phase-difference detection. The system is built with a DDS frequency generator, a voltage controlled current source, two high frequency instrumentation amplifiers, a phase-gain detector and a microcontroller unit. The software for the microcontroller is written and compiled on CodeVisionAVR C Compiler and the microcontroller is programmed on AVRStudio 4.

The accuracy and precision of the prototype device are checked against the HP 4284A LCR meter using different RC test loads. The results show that the overall percentage error averages of the real and imaginary parts of the complex impedance are 0.80 % and 1.78 % respectively.

The Cole-Cole diagrams are generated to obtain the Cole parameters, R_0, R_∞, f_c and α that give valuable information about the physiological status of biological tissues. Those parameters are also checked against the LCR meter. The percentage errors of α are found to be high due to relatively high phase-difference detection errors.

Keywords: bioimpedance, magnitude-ratio and phase-difference detection, direct digital synthesis (DDS), Cole-Cole plot, Cole-Cole parameters.

ÖZET

MİKRO DENETLEYİCİ KONTROLLÜ 100 kHz - 1 MHz ÇOKLU FREKANS BİYO-EMPEDANS ÖLÇÜM CİHAZI

Biyolojik sistemlerin patalojik ve fizyolojik durumlarının tespitinde kullanılan kompleks biyo-empedans analizi yöntemi, gün geçtikçe yaygınlaşmaktadır. Örnek olarak; vücut kütle endeksi, doku iskemisi, kanın tazeliği gibi durumların tespitinde biyo-empedans yöntemi yaygın olarak kullanılmaktadır.

Bu çalışmada sunulan cihaz, genlik-oranı ve faz-farkı tespiti prensiplerine dayanan, dört elektrodlu, çoklu frekans ve taşınabilir bir biyo-empedans ölçüm cihazıdır. Sistem bir adet frekans üreteci, voltaj kontrollü akım kaynağı, iki özdeş sinyal yükselticisi, faz ve genlik dedektörü ve bir mikro denetleyiciden oluşmaktadır. Mikro denetleyici yazılımı CodeVisionAVR C derleyicisinde oluşturulmuş ve derlenmiş, AVRStudio 4 programı ile mikro denetleyiciye yüklenmiştir.

Üretilen prototip cihazın doğruluk ve hassasiyeti, farklı RC test devrelerinden alınan ölçüm sonuçlarının HP 4284A LCR ölçüm cihazı ile yapılan ölçüm sonuçlarıyla kıyaslanması yolu ile sınanmıştır. Elde edilen sonuçlara göre karmaşık empedansın gerçek ve sanal bileşenlerinin hata yüzdelerinin ortalamaları % 0,80 ve % 1,78 olarak hesaplanmıştır.

Elde edilen ölçüm sonuçlarının Cole-Cole diyagramları çizilerek Cole parametreleri, R_0, R_∞, f_c ve α, elde edilmiştir. Biyo-empedans ölçümü sonuçlarının Cole-Cole diyagramında gösterilmesi ile dokuların fizyolojik durumları ile ilgili önemli sonuçlar elde edilebilir. Bulunan Cole parametreleri de LCR ölçüm cihazı ile karşılaştırılmıştır. Sonuçlar içerisinde, α değerlerinde faz-farkı tespitinde oluşan hatalardan kaynaklı olarak sapmalar olduğu gözlenmiştir.

Anahtar Sözcükler: biyo-empedans, genlik-oranı ve faz-farkı tespiti, doğrudan dijital

sentez (DDS), Cole-Cole diyagramı, Cole-Cole parametreleri.

TABLE OF CONTENTS

LIST OF FIGURES

LIST OF TABLES

LIST OF SYMBOLS

R	Resistance
X	Reactance
$\tilde{Z}$	Complex impedance
Z	Amplitude of the complex impedance
θ	Phase angle
Y	Admittance
G	Conductance
B	Susceptance
C	Capacitance
R_0	Resistance at zero frequency
R_∞	Resistance at infinite frequency
f_c	Characteristic frequency
α	A parameter showing the deviation from pure capacitance
V_S	Amplified voltage across the sample
V_R	Amplified voltage across the reference resistor
V_{MAG}	Magnitude ratio output of the phase-gain detector
V_{PHS}	Phase difference output of the phase-gain detector
L	Length
A	Cross sectional area
ρ	Resistivity coefficient
R_e	Extracellular fluid resistance
R_i	Intracellular fluid resistance
R_m	Cell membrane resistance
C_m	Cell membrane capacitance
ω	Angular frequency
τ	Time constant
ϕ	Depression angle of a Cole-Cole plot

LIST OF ABBREVIATIONS

BIMD	Bio-impedance measurement device
DDS	Direct Digital Synthesis
VCCS	Voltage controlled current source
IA	Instrumentation Amplifier
PGD	Phase-gain detector
DAC	Digital-to-Analog Converter
MCLK	Master clock
SCLK	Serial clock
FSYNC	Frequency Synchronization
SDATA	Serial data
RISC	Reduced instruction set computing
ADC	Analog-to-Digital Converter
IC	Integrated circuit
CMRR	Common mode rejection ratio

1. INTRODUCTION

Bioimpedance analysis is the analysis of the specific resistance and reactance of living tissues. In other words, it determines how the current passing through a biological cell is stopped or slowed down. Accurate measurements of impedance of biomaterials over a broad frequency range provide valuable information about the electrical properties of tissues or organs.

Below are some examples to bioimpedance applications:

- in-vivo muscle and tissue studies,
- electrode skin studies,
- dermatological applications,
- drug delivery rates,
- pacemaker development,
- blood cell analysis, monitoring of viral effects on cell structure,
- biotechnology research, food and pharmaceuticals [1].

The measurement of the resistance and reactance of the body simply depends on applying low level electrical currents ($<$1 mA) and monitoring the resulting electrical voltage.

There are many methods in measuring bioimpedance, each of which has advantages and disadvantages. The first thing to do is to figure out the parameters that are important for the measurements and choose the most appropriate method depending on these parameters which are the frequency coverage, measurement range, measurement accuracy, and ease of operation.

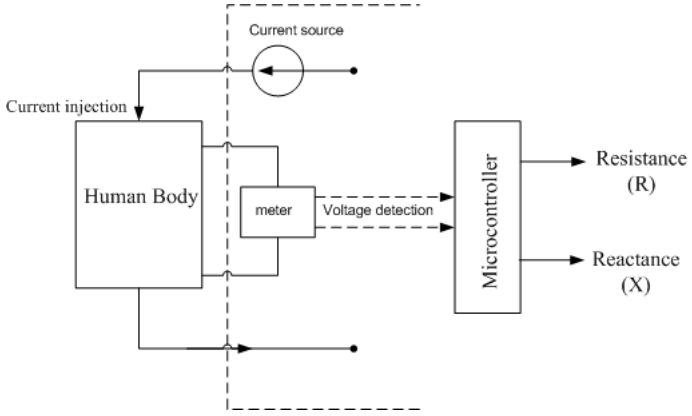

Figure 1.1 Bio-impedance measurement system.

The two basic bio-impedance measurement techniques are the Bridge method and the phase sensitive detector (PSD) method, using either two or four electrode systems. In both techniques, there are some difficulties imposed on the instrumentation those lead to changes or errors during the measurements and must be examined separately. Some of those are the frequency range of operation, accuracy of the measurement, safety while connecting to live subjects and the elimination of stray impedances due to cables and electrodes [2].

Although the bridge method had been traditionally the most popular method with its major advantage of high measurement resolution and accuracy, this method is time-consuming due to the need for bridge balance and not suitable where the impedance of the tissue changes rapidly during ongoing physiological processes [3].

Figure 1.2 is a simple diagram of how the bridge method works;

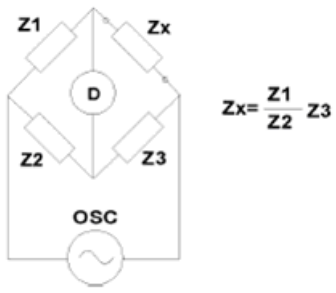

Figure 1.2 The bridge method [4].

When no current passes through the detector (D), the unknown impedance can be obtained by the relationship of the other bridge elements. Bridge method is mostly used in measurements up to frequencies of 300 MHz [4].

With the development of phase sensitive detectors, bio-impedance measurement circuits are mostly based on magnitude-ratio and phase-difference detection (MRPDD) principles. The most important difference between the PSD method and the other methods is that, the MRPDD method is based on the detection of relative amplitude and phase of two signals.

The complex impedance measurement may be done with two-electrode or four-electrode systems. However, in the two-electrode system, when an alternating current is passed through the electrodes, frequency dependent polarization impedance occurs at which results reflect both the impedance of the sample and the electrode-tissue interface [5].

Fortunately, the electrode-tissue interface can be eliminated by using the four-electrode technique: separate pair of electrodes are used for current injection and voltage detection. Since the voltage is measured with very high input impedance, practically no current flows through the voltage detecting electrodes. Electrode polarization is avoided and the contact impedance is eliminated from the measurement [3, 4, 5].

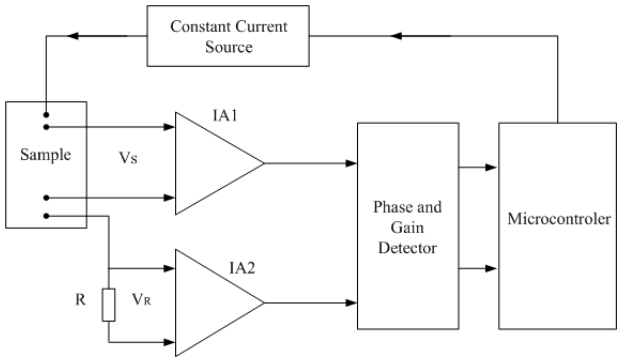

Figure 1.3 Block diagram of a PSD type bioimpedance analyzer.

The block diagram of a PSD type bio-impedance analysis system based on the MRPDD method is illustrated in Figure 1.3.

In Figure 1.3, R is the reference resistor connected in series with the sample and V_S and V_R are the amplified voltage differences across the measured impedance and the reference resistor, respectively. V_S and V_R are then compared in the phase-gain detector. The phase-gain detector produces two output voltages, namely V_{MAG} and V_{PHS}. V_{MAG} is the voltage proportional to the magnitude-ratio of the two input signals whereas V_{PHS} is proportional to the phase-difference between the input voltages. Then these two output voltages, V_{MAG} and V_{PHS}, are sent to the microcontroller unit that performs mathematical calculations in order to find the unknown complex impedance.

2. THEORY AND METHOD

2.1 Electrical Impedance

Electrical impedance is a complex quantity and consists of a real part (resistance, R), and an imaginary part (reactance, X). When an alternating current is applied through a biological tissue, the resistive opposition is caused by the sample itself, whereas the reactive opposition is due to the capacitive characteristics of the membranes, tissue interfaces, and nonionic tissues.

The complex impedance can be expressed in two different notations: The Cartesian Form:

$$\tilde{Z} = R + jX \tag{2.1}$$

The Polar Form:

$$\tilde{Z} = Ze^{j\theta} \tag{2.2}$$

In polar form, Z is the amplitude of the complex impedance and phase angle θ is the time delay between the stimulating current and the voltage generated by that current. The mathematical relationship between Z, R and θ is shown in Figure 2.1.

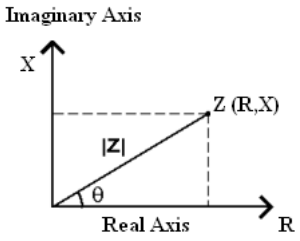

Figure 2.1 Graphical representation of the complex impedance plane.

$$Z = R + jX \tag{2.3}$$

$$Z = |Z|cos(\theta) \tag{2.4}$$

$$X = |Z|sin(\theta) \tag{2.5}$$

$$|Z| = \sqrt{R^2 + X^2} \tag{2.6}$$

In some cases, the reciprocal of the impedance, which is called the admittance, is more expedient. For,

$$Y = \frac{1}{Z} = \frac{1}{R + jX} \tag{2.7}$$

$$Y = G + jB \tag{2.8}$$

where Y represents the admittance, G conductance and B susceptance. Impedance expression is mostly preferred for cases where the resistive and capacitive elements are connected in series. However, if those elements are connected in parallel, it is better to use admittance representation for easiness. Figure 2.2 and 2.3 focus on these two representations.

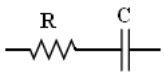

Figure 2.2 Real and imaginary components in series.

Impedance representation is better to express;

$$Z = R + jX \tag{2.9}$$

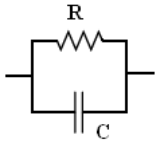

Figure 2.3 Real and imaginary components in parallel.

Impedance representation makes the expression complex;

$$Z = \frac{jRX}{R + jX} = \frac{RX^2}{R^2 + X^2} + j\frac{R^2X}{R^2 + X^2} \tag{2.10}$$

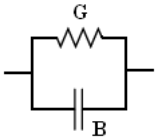

Figure 2.4 Real and imaginary components in parallel.

With the admittance representation, the expression gets simpler;

$$Y = G + jB \tag{2.11}$$

2.2 Bio-impedance Measurements

Biological organisms are made up of tissues and cells those are electrically resistive and reactive elements and connected in both series and parallel to each other. When an alternating current of a certain frequency is applied to a biological sample, each element of the sample reacts different to this flow of current depending on their electrical properties. The cell, which is the smallest structural and functional unit of a living organism, can be modeled as a combination of resistive and capacitive elements. The extracellular and intracellular fluids behave like resistors whereas cell membrane, which is surrounding the cell, is not only highly resistive but also capacitive. The cell structure of a tissue and response of the tissue to an excitation current are as follows,

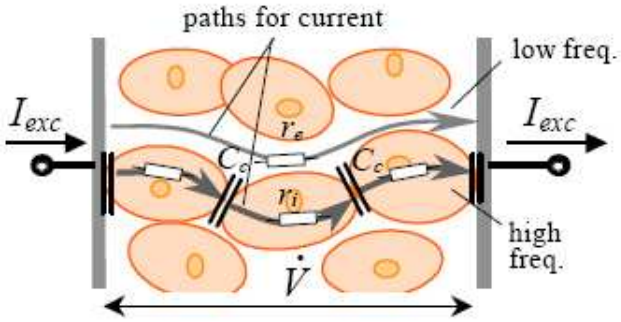

Figure 2.5 Tissue cell structure and bio-impedance formation [6].

One another important factor affecting the response of cells to a flow of current is the frequency. Frequency dependency is common for not only biological structures, but also all real-world components, since they are neither purely resistive nor purely reactive [7]. Figure 2.6 shows the characteristics of a pure resistor and a real resistor due to change in frequency.

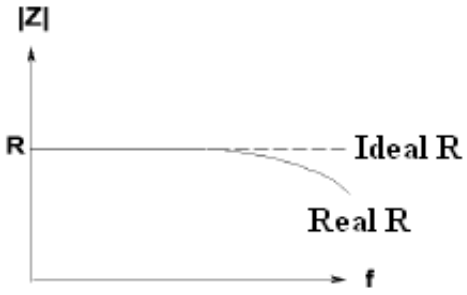

Figure 2.6 Frequency responses of ideal and real resistors [7].

When electrical current flows through a tissue, the path of the current changes due to frequency. At low frequencies, current travels in between individual cells. However, when the frequency increases, the cell membrane is short circuited and current penetrates through the cells.

To understand the physiological meanings of bio-impedance measurement results, researchers have been modeling biological units, i.e. cells, tissues, organs or the whole body, according to their electrical properties.

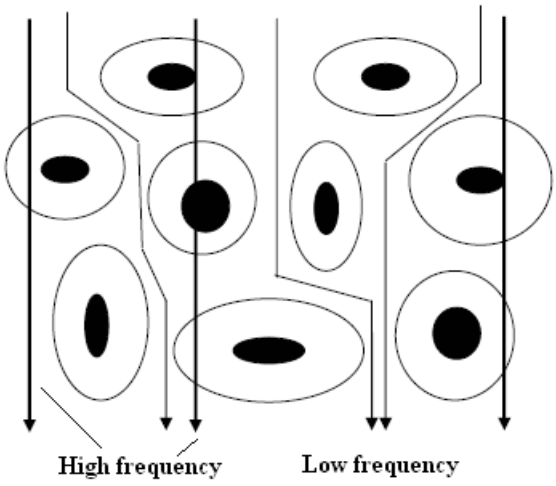

Figure 2.7 At high frequencies, current travels along straight bold lines. At low frequencies, current travels along thin lines.

If the body is assumed to be a simple geometrical system, namely a conductive cylinder, the resistance of the body would be proportional to its length and inversely proportional to its cross-sectional area.

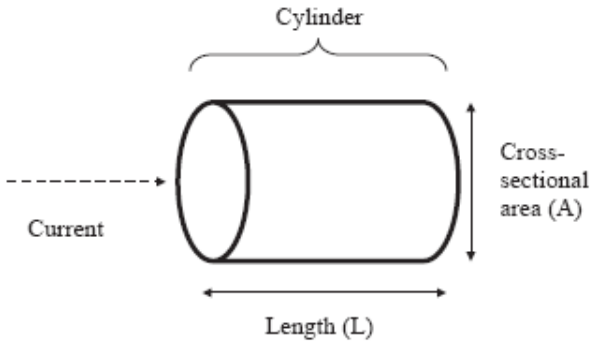

Figure 2.8 Cylindrical model of the body in order to figure out the relationship between resistance and geometry [8].

The resistance of such a conductive uniform cylinder with its length L and cross-sectional area A is,

$$R = \frac{\rho L}{A} = \frac{\rho L^2}{V} \tag{2.12}$$

where ρ is the resistivity coefficient of the material and V is the volume. However,

because of the fact that, body is not a uniform cylinder, errors occur due to variations in the resistivity of the body parts and variations in the shape of the body and body segments [8].

When a single cell is examined and modeled as an electrical circuit, the characteristic behaviors of intracellular fluid, extracellular fluid and cell membrane can be given as below,

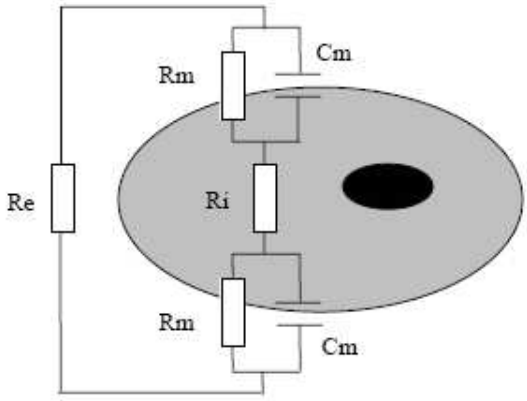

Figure 2.9 Electrically equivalent circuit model of a single cell.

where, R_e represents the extracellular fluid resistance, R_i is the intracellular fluid resistance, R_m is the membrane resistance and C_m is the membrane capacitance. This model may be simplified to four element and three element models as illustrated in Figure 2.10.

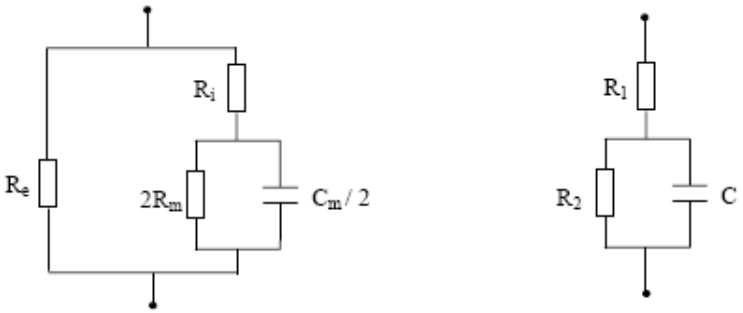

Figure 2.10 The four element and three element models of a single cell.

2.3 Cole-Cole Representation of the Complex Impedance

The complex series impedance of a single cell can be represented by the Cole-Cole plot, which is the depressed plot of the imaginary component against the real component of the impedance at different frequencies [9]. The Cole-Cole representation of the impedance provides the determination of the Cole parameters, namely R_0, R_∞, α and f_c, where R_0 is the resistance at zero frequency, R_∞ is the resistance at infinite frequency and f_c is the characteristic frequency [10]. The deviation from the pure capacitance is given by the experimental parameter α, which has a value between 0 and 1 ($\alpha = 1$; pure capacitance) [11]. The characteristic frequency of a RC element is the frequency at which the phase difference reaches its peak [12].

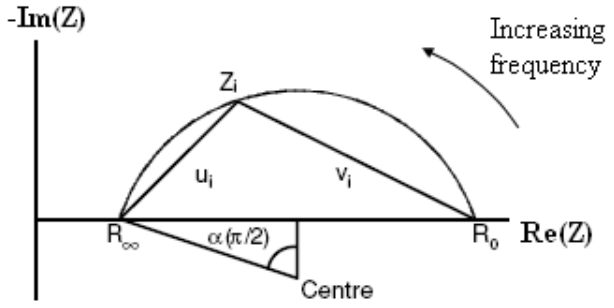

Figure 2.11 The depressed Cole- Cole plot [12].

Measuring the impedance at zero frequency is important because at this frequency the cell membrane acts like an insulator and electrical current can not penetrate into the cells. Therefore, the value at zero frequency represents the impedance of the extracellular fluid alone. At infinite frequency on the other hand, reactance of cell membrane capacitance approaches zero and the overall impedance can be thought as the impedance of extracellular fluid connected in parallel with the intracellular fluid [10, 11, 12].

Although impedance measurements at zero and infinite frequencies are impossible in practice, measuring the impedance in a range of frequencies from very low up to very high and then modeling the results in a Cole-Cole plot provides the determination of these parameters.

In 1940, Cole proposed the equation (2.13) to describe the impedance of biological tissues [12]. The Cole-Cole parameters satisfy this equation.

$$Z = R_\infty + \frac{R_0 - R_\infty}{1 + (jw\tau)^\alpha} \tag{2.13}$$

where $w = 2\,\pi f$ and τ is the time constant. When these parameters are once obtained from the complex impedance measurements, then the membrane capacitance C_m can be calculated easily from

$$C_m = \frac{1}{2\pi f_C (R_0 + R_\infty)^{\frac{1}{1-\alpha}}} \tag{2.14}$$

The cell has a single time constant and the plot is a semicircle of a radius equal to (R_0 - R_∞)/2 and intercepts the real axis at R_0 and R_∞ [12].

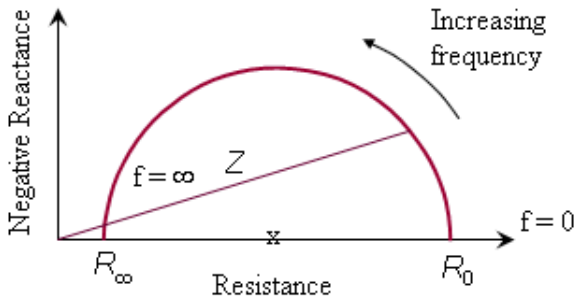

Figure 2.12 The Cole- Cole plot for complex impedance with a single time constant.

When complex impedance of a biological tissue is shown on the Cole-Cole plot, the center of the depressed circle is located below the real axis. The depression angle ϕ is equal to $\alpha\pi/2$ radians.

3. DESIGN PRINCIPLES

In this study, a four-electrode, adjustable frequency bio-impedance measurement device is designed and a prototype is built. The system is based on the principles of magnitude-ratio and phase-difference detection. The calibration measurements with resistors and RC circuits are done with the designed device and a commercial LCR meter HP 4284A. The results of the device are tested against the LCR meter in order to test the accuracy and precision of the device.

3.1 Device Block Diagram

The device is made up of a sine-wave generator, a voltage controlled current source, two identical instrumentation amplifiers, a phase-gain detector and a microcontroller unit.

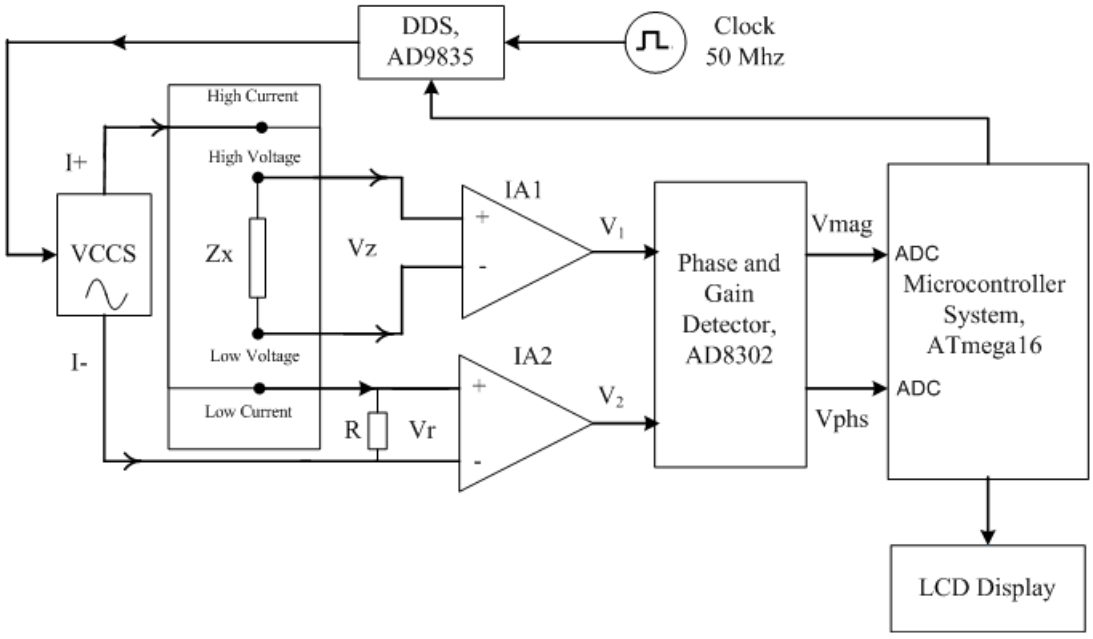

Figure 3.1 Block Diagram of the device.

In Figure 3.1, DDS stands for Direct Digital Synthesis, which is a digital high frequency sine-wave generation technique, VCCS is the voltage controlled current source

and IA1 and IA2 are the instrumentation amplifiers. V_Z is the resulting potential difference across the sample and V_R is the resulting potential difference across a known reference resistor.

The high frequency AC voltage, which is generated by the DDS, is transformed into a constant current of less than 1mA, by the voltage controlled current source. The constant current is then applied to the sample under test, via symmetrical current electrodes and to the reference resistor. The voltage across the sample is amplified by the instrumentation amplifier IA1. The voltage across the reference resistor is amplified by another instrumentation amplifier IA2 that is identical with IA1. The amplified voltages are then detected by the phase-gain detector (PGD). Phase and gain detection by using an IC has several advantages compared to many other methods because of its rapidity in measurements and simplicity of design and operation [13]. The outputs of the PGD are connected to the microcontroller unit that performs the complex impedance calculations. The microcontroller also adjusts the frequency of the generated signal by DDS and controls the LCD unit displaying the measurement results, namely Resistance (R), Reactance (X) and the Cole-Cole parameters.

3.1.1 Sine-wave Generator

Direct digital synthesis is a method for producing an analog waveform, usually a sine wave, by generating a time varying digital signal and then performing digital to analog conversion. Since the waveforms produced with DDS are digital, it is easy to produce fine resolution and broad range of frequencies [14]. With the improved technology, DDS integrated circuit chips are available, which can generate waveforms of frequencies less than 1 Hz up to 400 MHz. Currently, in multi-frequency systems, DDS is the best choice of signal generation in terms of low cost, low power consumption, fast settling time, low noise and wide bandwidth.

The main components of a DDS chip are a phase accumulator, a means of phase-to-amplitude conversion (often a sine look-up table), and a digital to analog converter

(DAC). The signal frequency depends on the reference clock frequency and the binary number programmed into the frequency register. The input of the phase accumulator is provided by the binary number in the frequency register. Then, the DAC converts that number to the corresponding amplitude of voltage or current [14].

The DDS system used in this design is based on the integrated circuit AD9835. AD9835 is a low power, frequency programmable fully integrated numerically controlled oscillator employing a phase accumulator, a COS Look-Up Table and a 10-bit D/A converter integrated on a single CMOS chip [15]. The AD9835 has a standard serial interface that allows the device to interface directly with several microprocessors. The AD9835 device requires one reference clock, one low precision resistor and eight decoupling capacitors that provide digitally created sine waves up to 25 MHz [15]. The frequency of the output signal is determined by the following equation with the 32-bit frequency register;

$$f_{OUT} = \frac{f_{CODE}}{2^{32}} f_{CLOCK} \tag{3.1}$$

where f_{CODE} is a number in FREQ and f_{CLOCK} is the frequency of the clock source [15]. In this design, since the clock frequency is 50 MHz, a resolution of 0.01 Hz can be achieved.

The AD9835 receives the clock frequency with the MCLK pin, which is the digital clock input of the chip. DDS output frequencies are expressed as a binary fraction of the frequency of MCLK [10]. The three pins connected to the ATmega16 are the SCLK, SDATA and FSYNC pins. SCLK pin is the logic input pin of the AD9835 at which the data is clocked into the chip. SDATA is the serial data input pin that the 16-bit serial data is applied to. When the data synchronization logic input pin FSYNC is taken low, the internal logic is informed that a new word is loaded into the device.

3.1.2 Voltage Controlled Current Source

The difficulty of building a current source for a bio-impedance measurement system is to design of a constant current source at which the output current will not change when the load resistance is changed.

The current source presented in this study is a high output impedance current source based on the dual transconductance amplifier CA3280. The CA3280 has all the generic characteristics of an operational voltage amplifier with the exception of that the output of the IC is current but not voltage [16]. The finite output impedance of the current source can cause the actual current delivered to the load to be lower than the current produced by the source.

3.1.3 Instrumentation Amplifiers

In an ideal four-probe impedance analyzer, the input impedance of the voltage detection system is infinite, whereas it is finite in real systems. For this high input impedance requirement, the AD8130, which is a low noise, very high input impedance (1 MΩ differential) differential to single ended amplifier is used. The amplifiers are used as instrumentation amplifiers because of the extremely high common mode rejection ratio (CMRR) of the IC at high frequencies [17].

The gains of the instrumentation amplifiers are adjusted as 4.75 by considering the output values of the buffer circuits that follow the amplifiers and send the voltages to the next element, phase-gain detector.

3.1.4 Phase - Gain Detector

The phase-gain detector is the most important part of the complex bio-impedance measurement system. It is based on the AD8302, which is a fully integrated system

for measuring gain-loss and phase difference in various applications. The input signals for the AD8302 range for amplitudes from -60 dBm (316 μV_{PEAK}) to 0 dBm (316 mV_{PEAK}) in a 50 Ω system [18].

The phase-gain detector design in this study consists of two parts, the input buffer and the AD8302.

3.1.4.1 Input Buffer The input buffer circuit based on the dual high frequency op-amp THS3062 (Texas Instruments, Dallas, Texas 75243, USA) is used in order to carry the output signals of the instrumentation amplifiers to the inputs of AD8302 and match the 50 Ω input impedance of the AD8302.

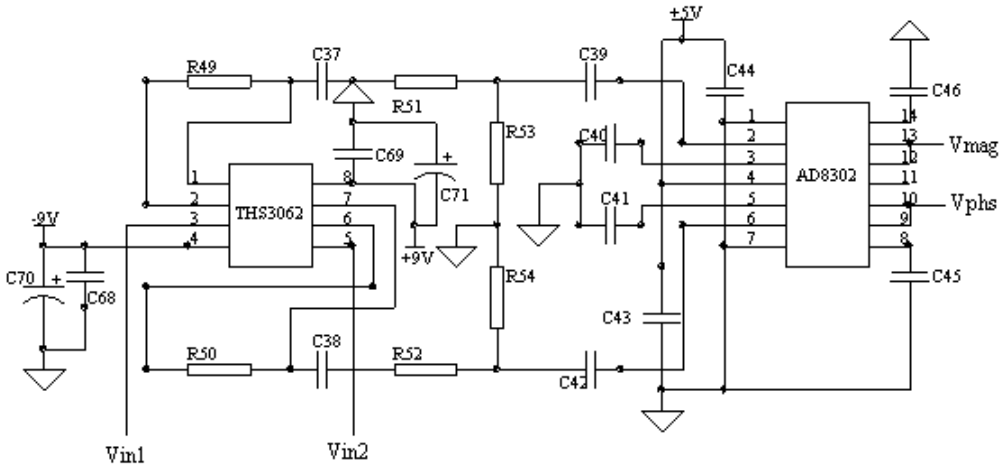

Figure 3.2 Circuit of the PGD.

The buffer circuit, on the left hand side in Figure 3.2, consists of THS3062, which is a high speed low output impedance unity gain amplifier, and voltage attenuators with and resistors. The aim of using voltage attenuators is to limit the amplitude of the signal between 316 μV_{PEAK} and 316 mV_{PEAK}. The two input voltages, V_{in1} and V_{in2} are the output voltages of the instrumentation amplifiers.

3.1.4.2 AD8302 The AD8302 comprises a phase detector and a pair of closely matched demodulating logarithmic amplifiers each in the range of ± 30dB. Logarithmic amplifiers provide a logarithmic compression function that converts the AC input signal levels to a compact decibel-scaled DC output. AD8302 takes the difference of the two signals in the output of the log amps that are driven by the input signals. Since subtraction in the logarithmic domain corresponds to a ratio in the linear domain, the mathematical formula of the gain operation can be defined as,

$$V_{MAG} = R_F I_{SLP} log(\frac{V_{INA}}{V_{INB}}) + V_{CP} \tag{3.2}$$

where V_{INA} and V_{INB} are the input voltages, V_{MAG} is the output voltage corresponding to the magnitude difference, V_{CP} is the central point voltage and $R_F I_{SLP}$ is called the slope voltage, which is a fundamental characteristic of the log amp.

The phase detector uses a fully symmetric structure with respect to its two inputs to maintain balanced delays along both signal paths. The phase detection operation is mathematically defined as,

$$V_{PHS} = -R_F I_\theta(|(\theta_1 - \theta_2)| - 90) + V_{CP} \tag{3.3}$$

where $R_F I_\theta$ is the slope of the phase function, (θ_1-θ_2) is the phase difference of the two input voltages and is the phase output voltage corresponding to the phase difference of degrees.

For the gain function, the slope represented by $R_F I_{SLP}$ is 600 mV/decade, for the phase function the slope represented by $R_F I_\theta$ is 10 mV/degree and the reference voltage adjusted for 0 dB gain and 0 degree phase difference is 900 mV. So the gain and phase functions may be defined as,

$$V_{MAG} = 600 log(\frac{V_{INA}}{V_{INB}}) + 900 \tag{3.4}$$

$$V_{PHS} = -10(|(\theta_1 - \theta_2)| - 90) + 900 \tag{3.5}$$

Figure 3.3 and Figure 3.4 are the idealized transfer characteristics for the gain and phase measurements [18].

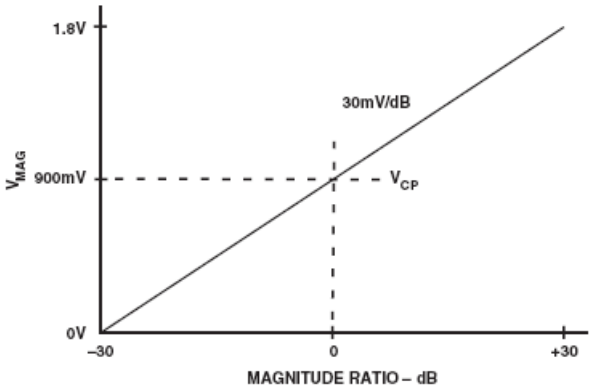

Figure 3.3 Transfer characteristics of the gain function [18].

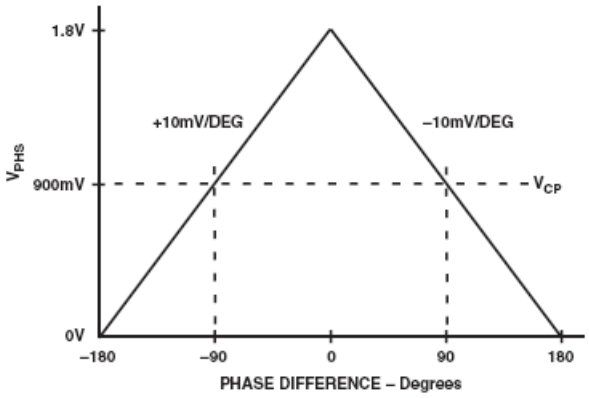

Figure 3.4 Transfer characteristics of the phase function [18].

The magnitude and phase difference of the voltages can be determined from the above equations as follows,

$$\frac{V_{INA}}{V_{INB}} = 10^{\frac{V_{MAG}-900}{600}} \tag{3.6}$$

$$\theta_1 - \theta_2 = -(\frac{900 - V_{PHS}}{10}) + 90 \tag{3.7}$$

3.1.5 Microcontroller System

The ATmega16 (Atmel Co., San Jose, California, USA) is a low power 8-bit microcontroller based on the RISC architecture. It is the key component of the system presented in this thesis because of its leading functions on the other components of the device and features used for performing the necessary operations. The functions of the ATmega16 in this system are;

- adjustment of the frequency and phase of the sine-waves generated by the DDS frequency generator by communicating with the IC AD9835,
- ADC operation in order to obtain the binary numbers that are used in the calculations of the unknown impedance,
- control of the LCD unit to display the measurement results.

When the power switch of the device is on, the ATmega16 becomes active starts its initialization process. The initial conditions are adjusted by the software created in "CodeVisionAVR" C Compiler and the ATmega16 is programmed on "AVRStudio 4". ATmega16 includes 1 Kbytes of RAM at which the operation results are stored until the power switch is off. In addition to the RAM, the 16 Kbytes of program flash memory, which enables the storage of the code written for the microcontroller, is an enough size of memory for the present software.

3.1.6 Power Supply

The active components used in this design require different DC power supplies, namely $\pm$ 9V and $\pm$ 5V. $\pm$ 9V supply voltages can be derived from two 9V batteries, whereas two voltage regulators, namely LM7805 and LM7905 are used in order to produce $\pm$ 5V.

The typical application schematics of these regulators are as given in the Figure 3.5.

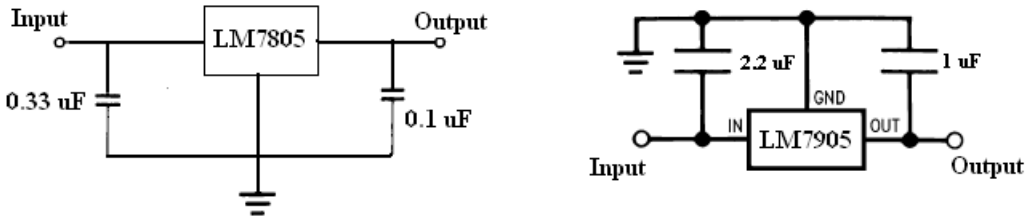

Figure 3.5 LM7805 and LM7905 voltage regulators.

3.2 The Microcontroller Code

The microcontroller code consists of two main parts, initialization and operation. The initializing part and operating part of the ATmega16 are adjusted due to the pin connections and functions. When the power switch of the device is on, the ATmega16 first initializes its ports and then waits for the user to start the measurements.

3.2.1 Initialization

3.2.1.1 Port Initializations The four ports of the microcontroller, namely PORTA, PORTB, PORTC and PORTD are set to logic 0 and their data direction registers, namely DDRA, DDRB, DDRC and DDRD are set due to their functions.

PORTA is the A/D Converter (ADC) port of the ATmega16. The first three pins of this port PA0, PA1 and PA2 are set as output, because these pins are connected to the SCLK, SDATA and FSYNC pins of the DDS frequency generator IC AD9835. These pins are used to provide communication between ATmega16 and AD9835 during sine-wave generation at desired frequency. The three logic input pins of the AD9835 receive data from these output pins of the ATmega16.

The fourth and fifth pins of the ADC port, PA3 and PA4 are set as input, since these two pins used as the analog to digital converters of the microcontroller. When the phase and gain detector IC, namely AD8302, sends the output signals to the ATmega16, these two analog DC voltages are converted to their digital equivalents according to the ADC reference voltage of the ATmega16, which is 2.56 Volts. The 10-bit ADC of the microcontroller makes the ADC conversion operation according to the equation,

$$\frac{V_{REF}}{2^{10}} = \frac{2.56}{1024} = 2.5mV \tag{3.8}$$

This means that, each input is divided into fractions of 2.5 mV and converted to its digital equivalent value in the ADC ports.

The two pins of the ADC port, PA6 and PA7 are connected to two switches, which are used to increase and decrease the frequency of the signal. Therefore these three pins are set as input. PORTB is an 8-bit, bi-directional I/O port. The first pin of this port, PB0 is set as input since it is connected to a third switch, which is responsible to give command to the ATmega16 to start the measurement. The other seven pins of PORTB are not connected to anything and set as output and to logic 0 to avoid noise.

PORTC is the LCD port of the ATmega16. Therefore this port is completely set to LCD display interface.

PORTD is not connected, so all the pins are set as output.

PORTA 0: Connected to the SCLK pin of the AD9835 and set as output.

PORTA 1: Connected to the SDATA pin of the AD9835 and set as output.

PORTA 2: Connected to the FSYNC pin of the AD9835 and set as output.

PORTA 3-4: Connected to the magnitude ratio and phase difference output pins of the AD8302 phase-gain detector. These pins are used as A/D converters and are set as input.

PORTA 6-7: These pins are connected to the frequency decrease and increase switches in order to change the frequency of the sine-wave, therefore set as input. The two buttons increase and decrease the frequency 100 kHz according to the command written in the software.

PORTB 0: This pin is connected to the trigger button, which starts the measurement and calculation processes. So it is set as input.

PORTB 1-7: These pins are not connected, so they are set as output in order to avoid noise.

PORTC: Connected to the LCD, therefore set as the LCD display interface.

PORTD: This port is not connected to any components and all pins are set as output.

Table 3.1
The port initializations of the microcontroller.

PORT	**A**	**B**	**C**	**D**
Output	0000 0000	0000 0000	0000 0000	0000 0000
DDR	0010 0111	1111 1000	1111 1111	1111 1111

3.2.1.2 Analog to Digital Converter The ADC converts an analog input voltage to a 10-bit digital value through successive approximation. The AREF pin must either be connected to AVCC or an internal 2.56 V reference voltage. In this design, 2.56 V internal voltage reference is selected and the AREF pin is decoupled by 10 nF capacitor in order to avoid noise.

3.2.1.3 LCD Display For the initialization of the LCD display the CodeVision C compiler embedded function "lcd_init()" is used. The LCD unit used in this design is a 2x16 LCD display with 2 rows and 16 columns. Since the number of columns is accepted as parameters in the LCD initialization function, the function is used as "lcd_init(16)".

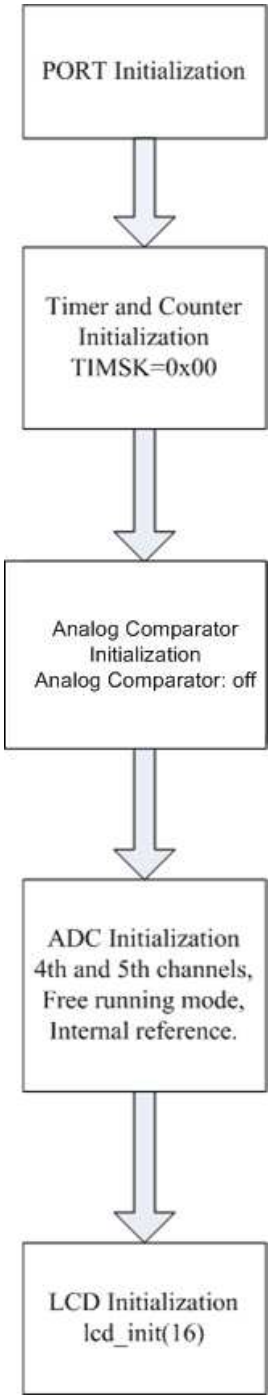

Figure 3.6 Initialization of the microcontroller.

3.2.2 Operation

After finishing the initialization process, the microcontroller sends commands to the DDS frequency generator AD9835 to generate an initial sine-wave of 100 kHz. Following the generation of the 100 kHz signal, the microcontroller sends data to the LCD unit in order to display the value of the generated frequency. The first pin of PORTC of the ATmega16 is connected to the Read/Write (R/W) input of the LCD. This pin decides on the mode of operation, whether READ or WRITE. The operation mode is always WRITE, so the LCD displays the frequency of the generated signal.

The "Trigger button", which is connected to PORTB 0, is used to start the measurement. When this button is pushed, the ADC pins of the ATmega16 calculate the average of the DC input voltages, which are the magnitude ratio (V_{MAG}) and phase difference (V_{PHS}) outputs of the phase gain detector AD9835. In other words, ATmega16 receives the magnitude ratio and phase difference of the sample under test and the reference resistor.

When these two voltages are detected by the ATmega16, the microcontroller transforms these analog signals to their digital values by A/D conversion. For example, if the measured sample is purely resistive and its resistance is equal to the reference resistance, then the magnitude ratio and phase difference outputs of the phase gain detector are going to be; $V_{MAG} = 900\ mV$, $V_{PHS} = 1800\ mV$.

Then the A/D conversion will convert these voltages to; $V_{MAG} = 900\ \frac{1024}{2560} = 360\ mV$ and $V_{PHS} = 1800\ \frac{1024}{2560} = 720\ mV$

For the the unknown impedance calculation, equations derived from the calculations of V_{MAG} and V_{PHS} by the AD8302, are programmed into the ATmega16.

From the formulas 3.4 and 3.5, the unknown complex impedance Z_m and the

phase difference θ can be expressed as,

$$|Z_m| = R_s 10^{(\frac{V_{MAG}-900)}{600})} \tag{3.9}$$

$$\theta = -(\frac{900 - V_{PHS}}{10} + 90) \tag{3.10}$$

Therefore, the resistive and reactive components of the complex impedance are calculated as follows;

$$R = |Z_m| cos(\theta) \tag{3.11}$$

then,

$$R = R_s 10^{(\frac{V_{MAG}-900)}{600})} cos(\frac{V_{PHS}}{10} - 180) \tag{3.12}$$

and

$$X = |Z_m| sin(\theta) \tag{3.13}$$

$$X = R_s 10^{(\frac{V_{MAG}-900)}{600})} sin(\frac{V_{PHS}}{10} - 180) \tag{3.14}$$

Moreover, the ATmega16 makes the phase calculations due to the radiant equivalent of the phase difference. So the equations become,

$$R = R_s 10^{(\frac{V_{MAG}-900)}{600})} cos[(\frac{V_{PHS}}{10} - 180)\frac{2\pi}{360}] \tag{3.15}$$

and

$$X = R_s 10^{(\frac{V_{MAG}-900)}{600})} sin[(\frac{V_{PHS}}{10} - 180)\frac{2\pi}{360}] \tag{3.16}$$

As mentioned in the previous sections, the electrical properties of biological

systems are frequency dependent. The response of tissues against an electrical current changes when the frequency of the current changes. Therefore, electrical bio-impedance measurements are performed in multi frequency.

The frequency of the produced signal can be adjustment by using the "increase button" and "decrease button" those are connected to PORTA 6 and PORTA 7 pins of the ATmega16. However, in the current design, the measurements are taken automatically from 100 kHz to 1 Mhz. After the real and imaginary components of the complex impedance are measured, the results are saved in the RAM of the ATmega16 and displayed on the LCD. Then these two measurement results, namely resistance and reactance, are used in the calculation of the Cole-Cole parameters. The four Cole parameters (R_0, R_∞, f_c and α), extracellular fluid resistance, (R_e), intracellular fluid resistance (R_i) and the center points and radius of the Cole plot (x_c, y_c and r) are determined and displayed on the LCD. The actual circuit diagram of the measurement device is given in Figure 3.7.

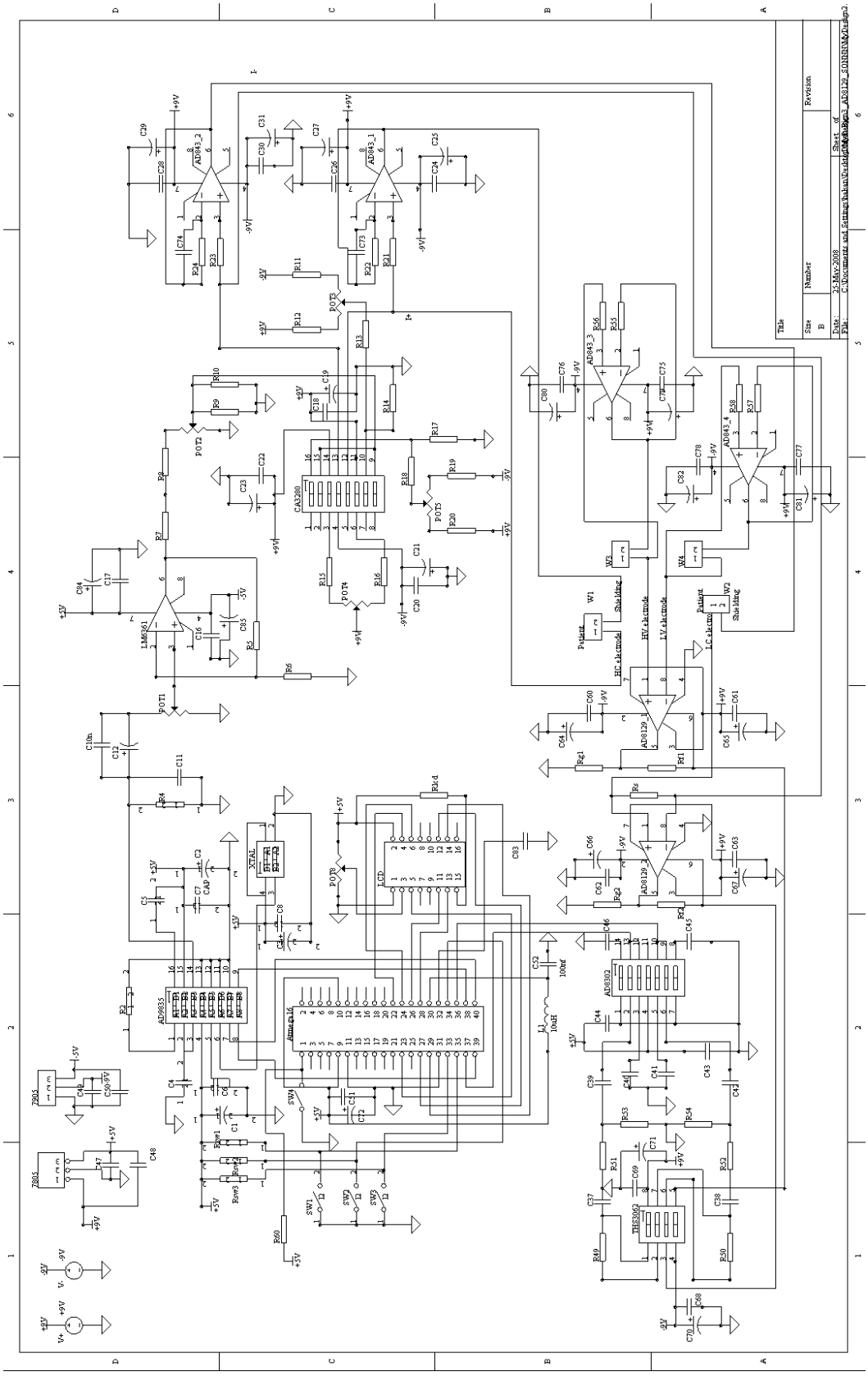

Figure 3.7 Actual circuit diagram of the measurement device.

4. RESULTS

Test measurements are performed to evaluate the accuracy and the precision of the device with reference to the HP 4284A LCR meter.

4.1 RC Measurements

As mentioned previously, the extracellular and intracellular fluids of a cell behave like resistors whereas the cell membrane has both the resistive and capacitive properties. According to this hypothesis, the test measurements are taken on single resistors and RC circuits that consist of two resistors and a capacitor as shown in the area framed by the dashed lines in Figure 4.1. The two 51 Ω resistors are used to simulate the resistance between the current input and voltage measurement electrodes [19].

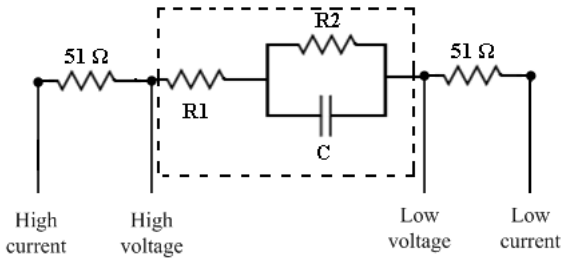

Figure 4.1 Four-terminal configuration of RC test circuits.

Test measurements are taken at 10 frequencies from 100 kHz to 1 MHz in 100 kHz increments. Initial measurements are performed on pure resistors. Then, complex impedances of three different RC circuits are measured to assess the precision and accuracy of the device.

4.2 Precision and Accuracy

4.2.1 Precision

Multi-frequency measurements are repeated for five times to test the repeatability of the device. Table 4.1 shows the results of the measurements on pure resistors.

Table 4.1
The results of measurements on resistors.

Resistances* **(Ω)**	**Average**	**% Error**	**STDEV**	**Coefficient of Variation**
100	100.07	0.07	0.63	$6.3\text{x}10^{-3}$
200	200.20	0.10	0.42	$2.1\text{x}10^{-3}$
328	328.13	0.04	1.36	$4.1\text{x}10^{-3}$
428	427.52	0.11	0.18	$4.1\text{x}10^{-4}$
718	718.40	0.06	0.46	$6.4\text{x}10^{-4}$
981	981.70	0.07	0.82	$8.4\text{x}10^{-4}$

* *Resistance values measured using the LCR meter.*

4.2.2 Accuracy

For the assessment of the accuracy of the impedance analyzer, measurements on three test circuits are taken with the designed bio-impedance measurement device (BIMD) and the HP 4284A LCR meter.

The resistor and capacitor combinations of the test circuits are as given in Table 4.2.

The real part of the complex impedance, namely the resistance, is decreasing with increasing frequency, as expected. On the other hand, the reactive part also tends to decrease with increasing frequency, depending on the characteristic frequency of the

Table 4.2
The results of measurements on resistors.

	R_1 (Ω)	R_2 (Ω)	C (nF)
Circuit 1	100	330	1
Circuit 2	200	500	10
Circuit 3	120	200	2.2

Table 4.3
Measurement results of Circuit 1.

Frequency	**Real (Z)**			**Imaginary (Z)**		
(kHz)	**BIMD**	**LCR meter**	**% Error**	**BIMD**	**LCR meter**	**% Error**
100	414.20	412.40	0.44	66.62	65.58	1.59
200	375.12	377.58	0.65	117.80	116.20	1.38
300	331.85	335.94	1.22	148.70	148.00	0.47
400	290.36	293.51	1.07	162.90	162.14	0.47
500	254.53	257.05	0.98	164.90	164.68	0.13
600	226.77	227.53	0.33	162.40	162.61	0.13
700	203.70	209.23	2.64	156.50	157.55	0.67
800	184.90	184.97	0.04	147.62	147.07	0.37
900	170.84	173.62	1.60	139.17	136.45	1.99
1000	160.36	158.27	1.32	131.62	130.04	1.22

RC circuit.

$$f_c = \frac{1}{2\pi RC} \tag{4.1}$$

The deviation observed in the imaginary component of the complex impedance is found to be caused by inaccurate detection of the phase difference between the current and voltage signals. This may be due to many factors affecting the measurements i.e. inadequate instrumentation, improper electrode application, the characteristic of the circuit or the stray capacitance of the cables [20].

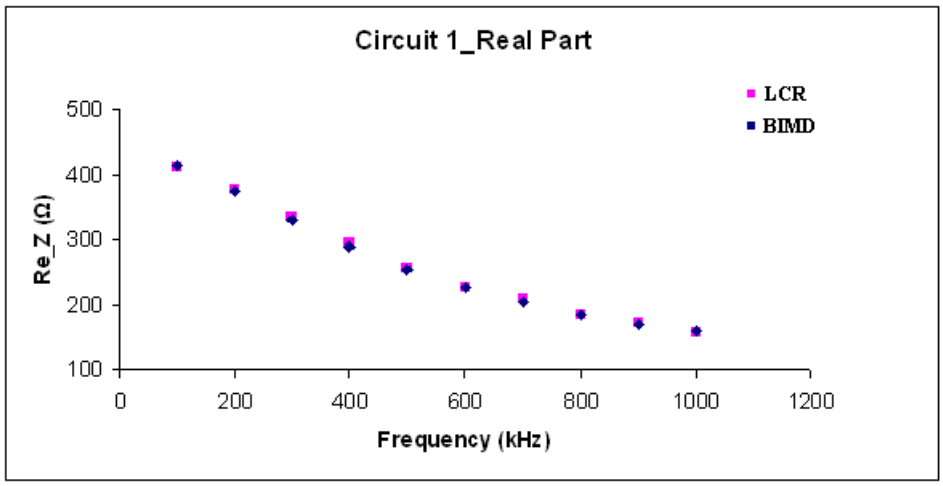

Figure 4.2 Real part results of Circuit 1.

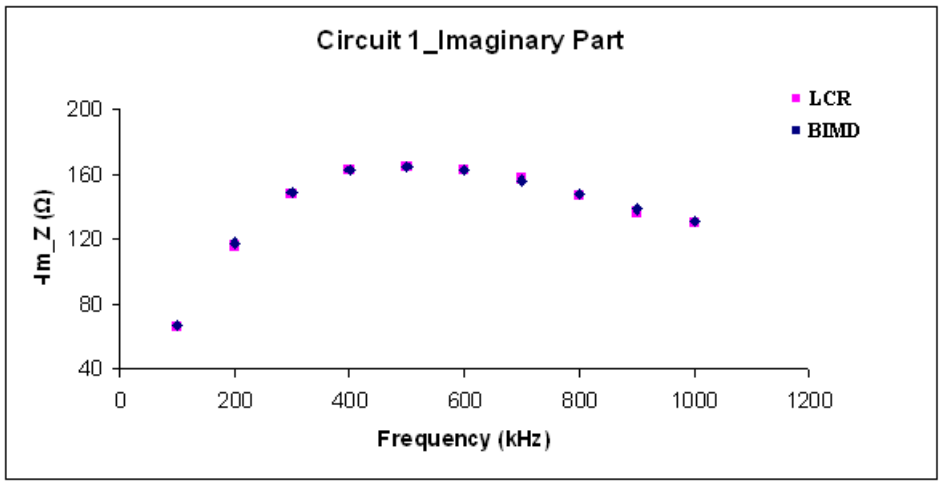

Figure 4.3 Imaginary part results of Circuit 1.

As mentioned in the previous sections, the AD8302 detects the magnitude ratio and phase difference of two AC signals. Although the AD8302 has a frequency range from 0 Hz up to 2.7 GHz, in practice it is designed particularly for radio frequency applications [13]. However, there is no alternative integrated chip available for phase-gain detection. Therefore AD8302 is used in this design for gain and phase detection.

With unity gain and zero phase difference between two AC signals, the AD8302 gives the two outputs $V_{MAG} = 900$ mV for magnitude ratio and $V_{PHS} = 1800$ mV for phase difference. However, as it is mentioned in the AD8302 datasheet, this ideal case

Table 4.4
Measurement results of Circuit 2.

Frequency	Real (Z)			Imaginary (Z)		
(kHz)	BIMD	LCR meter	% Error	BIMD	LCR meter	% Error
100	244.63	246.00	0.56	156.27	150.94	3.53
200	212.14	212.35	0.10	83.92	82.70	1.48
300	206.55	205.57	0.48	56.54	56.28	0.46
400	204.48	203.15	0.66	41.82	42.55	1.72
500	203.77	202.02	0.87	33.10	34.16	3.10
600	203.26	201.40	0.92	27.43	28.50	3.75
700	203.01	201.03	0.98	23.00	24.60	6.50
800	202.83	200.79	1.02	20.11	21.22	5.23
900	202.75	200.62	1.06	17.71	17.70	0.06
1000	202.70	200.51	1.09	15.91	16.16	1.55

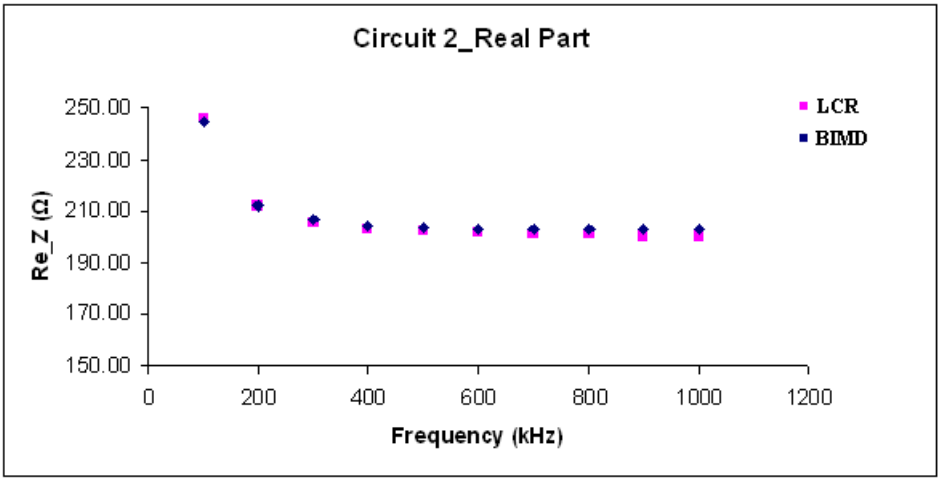

Figure 4.4 Real part results of Circuit 2.

is not always valid in real-life measurements.

According to the experimental studies on the AD8302 as shown on Figure 4.9 and 4.10, the magnitude output for unity gain of two signals is about 900 mV, whereas the phase difference output has a maximum at about 1800 mV [18].

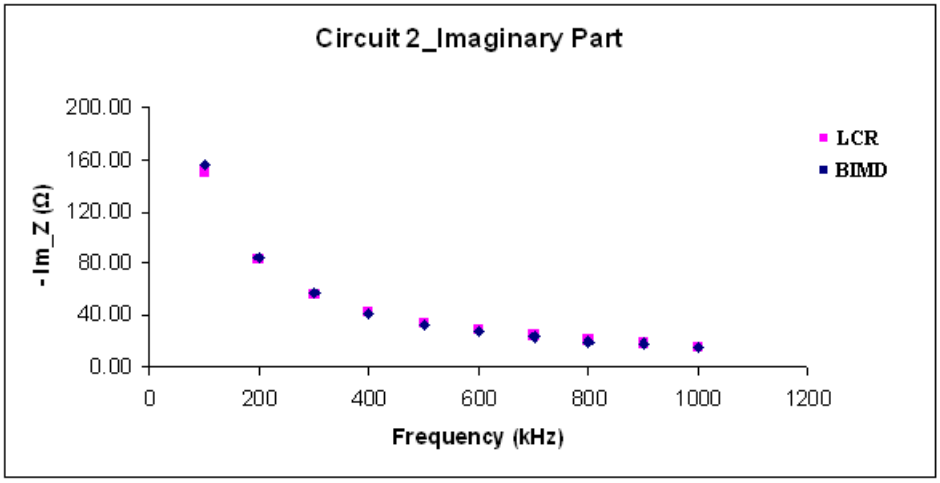

Figure 4.5 Imaginary part results of Circuit 2.

Table 4.5
Measurement results of Circuit 3.

Frequency	Real (Z)			Imaginary (Z)		
(kHz)	BIMD	LCR meter	% Error	BIMD	LCR meter	% Error
100	305.92	304.43	0.49	51.71	51.76	0.10
200	271.89	271.34	0.20	85.87	83.72	2.57
300	237.17	237.83	0.28	99.33	96.78	2.63
400	208.71	210.24	0.73	101.17	99.14	2.05
500	187.89	189.12	0.65	96.11	94.50	1.70
600	172.70	174.25	0.89	89.64	87.98	1.89
700	161.52	163.49	1.20	81.89	82.63	0.90
800	153.46	154.31	0.55	75.50	75.21	0.39
900	147.76	146.68	0.74	69.79	66.32	5.23
1000	142.95	143.42	0.33	64.05	63.90	0.23

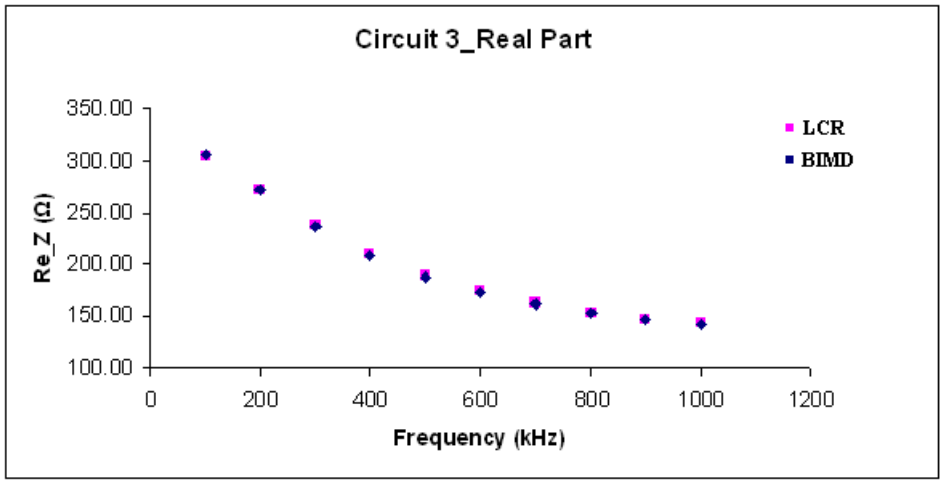

Figure 4.6 Real part results of Circuit 3.

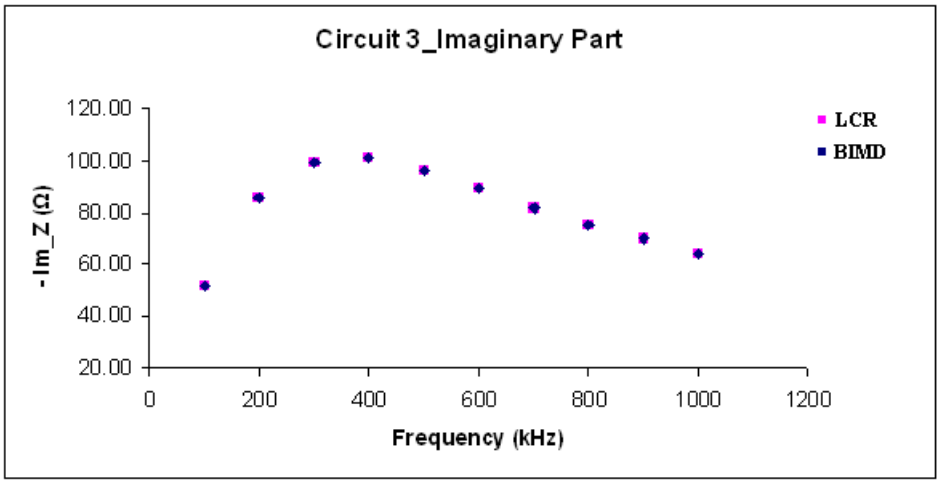

Figure 4.7 Imaginary part results of Circuit 3.

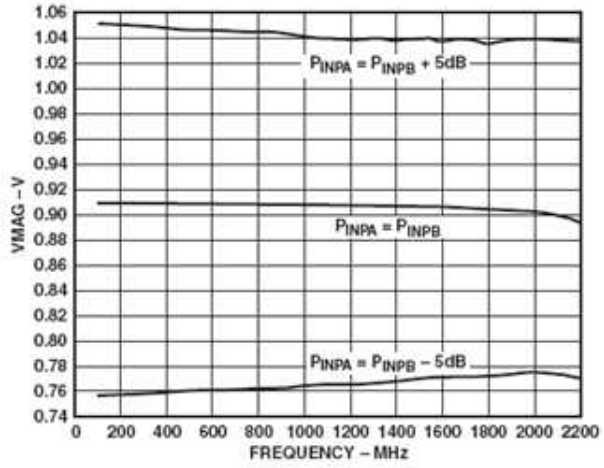

Figure 4.8 V_{MAG} output with change in frequency [18].

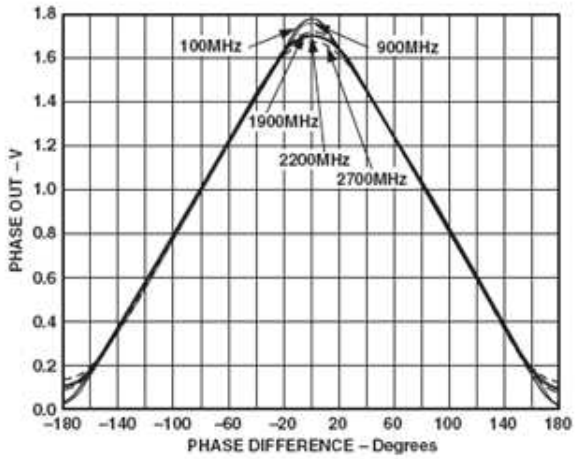

Figure 4.9 V_{PHS} output with change in frequency [18].

4.2.3 Cole-Cole Representation

The Cole-Cole diagrams of the results obtained by both the BIMD and the LCR meter are plotted. The plotting software is written on **MATLAB 6.5**.

The four Cole parameters (R_0, R_∞, f_c and α), extracellular fluid resistance, (R_e), intracellular fluid resistance (R_i) and the center points and radius of the Cole plot (x_c, y_c and r) are calculated from the measurement results.

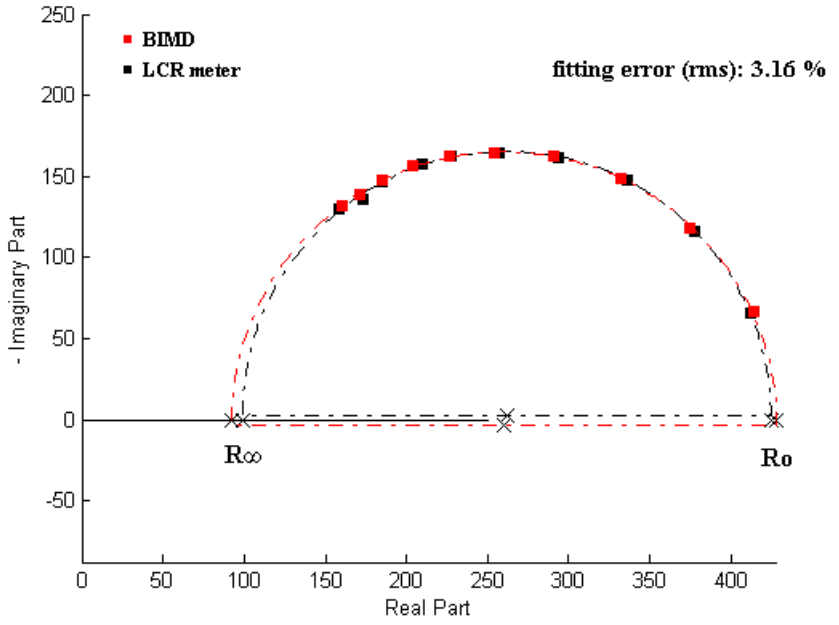

Figure 4.10 Cole-Cole plots of Circuit 1.

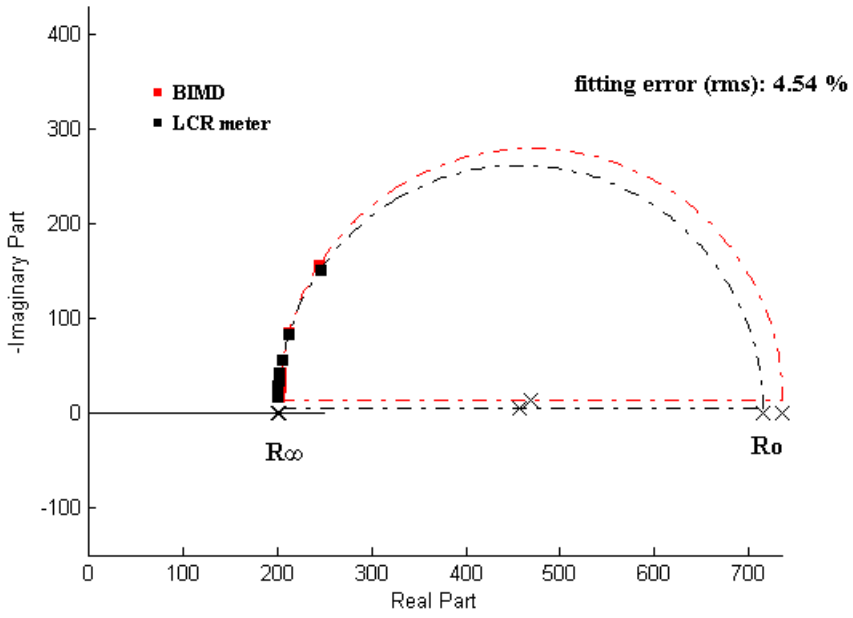

Figure 4.11 Cole-Cole plots of Circuit 2.

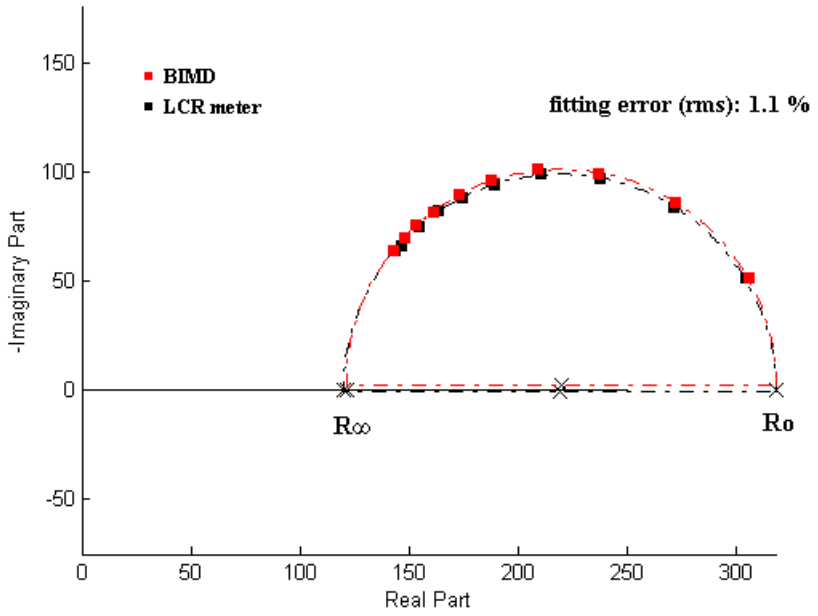

Figure 4.12 Cole-Cole plots of Circuit 3.

Tables 4.6, 4.7 and 4.8 compare those parameters obtained by the BIMD and LCR meter.

Table 4.6
The Cole parameters of Circuit 1 obtained by the BIMD and LCR meter.

Circuit 1	BIMD	LCR meter	% Error
$\mathbf{R}_o$	428.29	424.7	0.85
$\mathbf{R}_\infty$	91.752	98.668	7.01
α	0.012	0.009	24.31
$\mathbf{f}_c$	490	485	1.05
$\mathbf{R}_e$	428.29	424.7	0.85
$\mathbf{R}_i$	116.77	128.53	9.15

R_0 represents the impedance of the extracellular fluid (ECF) alone, since the cell membrane acts as an insulator at zero frequency. On the other hand, the reactance of cell membrane approaches zero at infinite frequency. Therefore, R_∞ represents the impedance of a parallel connection of extracellular fluid and intracellular fluid [10, 11, 12].

Table 4.7
The Cole parameters of Circuit 2 obtained by the BIMD and LCR meter.

Circuit 2	**BIMD**	**LCR meter**	**% Error**
$\mathbf{R}_o$	731.5	714.49	2.38
$\mathbf{R}_\infty$	203.2	200.32	1.44
α	0.03	0.01	189.91
$\mathbf{f}_c$	302	316	4.35
$\mathbf{R}_e$	731.5	714.49	2.38
$\mathbf{R}_i$	281.3	278.36	1.06

Table 4.8
The Cole parameters of Circuit 3 obtained by the BIMD and LCR meter.

Circuit 3	**BIMD**	**LCR meter**	**% Error**
$\mathbf{R}_o$	317.1	318.76	0.52
$\mathbf{R}_\infty$	122.5	119.87	2.19
α	0.0290	0.0027	977.07
$\mathbf{f}_c$	355	364	2.55
$\mathbf{R}_e$	317.1	318.76	0.52
$\mathbf{R}_i$	199.7	192.11	3.95

α is the parameter between zero and one that shows the deviation from pure capacitance ($\alpha = 1$; purely capacitive) whereas f_c is the characteristic frequency given in kHz.

Figure 4.13 The pictures of the measured parameters displayed on the LCD. (a) Adjusted frequency (b) Real and Imaginary parts of the complex impedance (c) Center coordinates of the Cole-Cole plot (d) R_0 and R_∞ (e) Chacteristic frequency (f) α.

5. CONCLUSION

In this study, a microcontroller based, multi-frequency, four-probe bio-impedance analyzer is designed and built. The device is based on the principles of magnitude-ratio and phase difference detection.

In order to test the precision and accuracy of the device, various measurements are taken from different resistors of known values and RC test circuits. The measurement results are compared with those of measurements taken by the reference device HP 4284A LCR meter.

The performance of the BIMD basically relies on the performance of the phase-gain detector chip AD8302. Although the AD8302 is an IC designed for radio frequency and intermediate frequency usage, it is the only available IC in the market that can be used for detecting the magnitude-ratio and phase difference of two signals without any other additional complex and expensive circuit components.

The measurement results figure out that the BIMD works precise and accurate. The overall percentage error averages of the real and imaginary parts of the complex impedance are 0.80 % and 1.78 % respectively.

The Cole-Cole diagrams of the results are plotted in order to obtain the Cole parameters. The Cole-Cole diagrams of BIMD and the LCR meter match with each other. The four Cole parameters, namely R_0, R_∞, f_c and α, gave reasonably good fit to the measured impedance spectra. However, percentage errors of α and y_c are obtained too high. These are caused by phase-difference detection errors of the device. Small deviations on the y axis of Cole plots resulted with high errors of α.

APPENDIX A. SPECIFICATIONS OF THE INTEGRATED CIRCUITS

A.1 ATmega16 - 8 bit Microcontroller

- High-performance, Low-power 8-bit Microcontroller
- Advanced RISC Architecture
  - 32 x 8 General Purpose Working Registers
  - Fully Static Operation
  - Up to 16 MIPS Throughput at 16 MHz
  - On-chip 2-cycle Multiplier
- Nonvolatile Program and Data Memories
  - 16K Bytes of In-System Self-Programmable Flash
  - In-System Programming by On-chip Boot Program
  - True Read-While-Write Operation
  - 512 Bytes EEPROM
  - 1K Byte Internal SRAM
- Peripheral Features
  - Two 8-bit Timer/Counters with Separate Prescalers and Compare Modes
  - One 16-bit Timer/Counter with Separate Prescaler, Compare Mode, and Capture Mode
  - Real Time Counter with Separate Oscillator
  - Four PWM Channels
  - 8-channel, 10-bit ADC
  - Byte-oriented Two-wire Serial Interface

- Programmable Serial USART

- Master/Slave SPI Serial Interface

- Programmable Watchdog Timer with Separate On-chip Oscillator

- On-chip Analog Comparator

- Special Microcontroller Features

  - Power-on Reset and Programmable Brown-out Detection

  - Internal Calibrated RC Oscillator

  - External and Internal Interrupt Sources

  - Six Sleep Modes: Idle, ADC Noise Reduction, Power-save, Power-down, Standby and Extended Standby

- I/O and Packages

  - 32 Programmable I/O Lines

  - 40-pin PDIP, 44-lead TQFP, and 44-pad QFN/MLF

- Operating Voltages

  - 2.7 - 5.5V for ATmega16L

  - 4.5 - 5.5V for ATmega16

- Speed Grades

  - 0 - 8 MHz for ATmega16L

  - 0 - 16 MHz for ATmega16

- Power Consumption @ 1 MHz, 3V, and 25°C for ATmega16L

  - Active: 1.1 mA

  - Idle Mode: 0.35 mA

  - Power-down Mode: 1 μA max

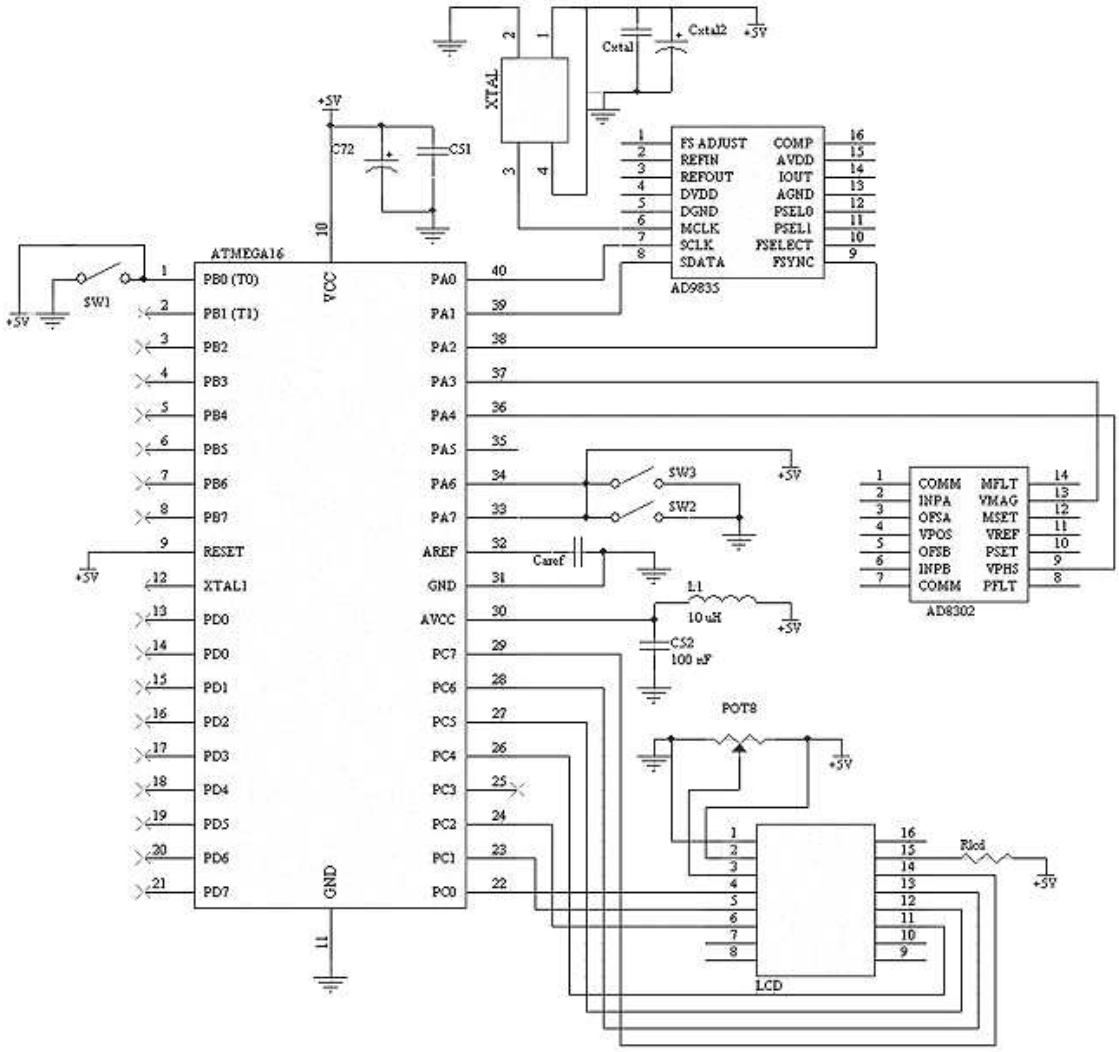

Figure A.1 Actual connection circuit of the ATmega16.

A.2 AD8302 - RF/IF Gain and Phase Detector

Table A.1
Specifications of the AD8302.

Parameter	**AD8302**	**Units**
OVERALL FUNCTION		
Input Frequency Range	0 - 2700	MHz
Gain Measurement Range	± 30	dB
Phase Measurement Range, ϕ_{IN} at INPA > ϕ_{IN} at INPB	± 90	degree
Reference Voltage Output	1.8 typ	V
MAGNITUDE OUTPUT, Pin VMAG		
Output Voltage Minimum, 20 x log(V_{INPA}/V_{INPB}) = 30 dB	30	mV
Output Voltage Maximum, 20 x log(V_{INPA}/V_{INPB}) = +30 dB	1.8	V
Center Point of Output (MCP), $V_{INPA} = V_{INPB}$	900	mV
Output Current	8	mA
Slew Rate, 40 dB Change, Load 20 pF||10 kΩ	25	V/μs
Response Time,		
Rise Time, Any 20 dB Change,	50	ns
Fall Time, Any 20 dB Change,	60	ns
Settling Time, Full-Scale 60 dB Change,	300	ns
PHASE OUTPUT, Pin VPHS		
Output Voltage Minimum, Phase Difference 180 Degrees	30	mV
Output Voltage Maximum, Phase Difference 0 Degrees	1.8	V
Phase Center Point, When $\phi_{INPA} = \phi_{INPB}$ ± 90°	900	mV
Output Current	8	mA
Slew Rate, 40 dB Change, Load 20 pF||10 kΩ	25	V/ms
Response Time,		
Any 15 Degree Change,	40	ns
120 Degree Change,	500	ns
POWER SUPPLIES		
Supply	2.7 - 5.5	V min - V max
Operating Current (Quiescent), V_S = 5V	21 - 27	mA

A.3 AD9835 - 50 MHz CMOS DDS

Table A.2
Specifications of the AD9835.

Parameter	AD9835B	Units
SIGNAL DAC SPECIFICATIONS		
Resolution	10	Bits
Update Rate (f_{MAX})	50	MSPS nom
IOUT Full Scale	4	mA nom
	4.75	mA max
Output Compliance	1.35	V max
DC Accuracy	50	MSPS nom
Integral Nonlinearity	± 1	LSB type
DDS SPECIFICATIONS		
Dynamic Specifications		
Signal-to-Noise Ratio	50	dB min
Total Harmonic Distortion	-52	dB_c max
Spurious Free Dynamic Range (SFDR)		
Narrow Band (± 50 kHz)	-72	dB_c min
Wide Band (± 2 MHz)	-50	dB_c min
Clock Feedthrough	-60	dB_c typ
Wake-Up Time	-60	dB_c typ
Power-Down Option	yes	
VOLTAGE REFERENCE		
Internal Reference @ +25°C	1.21	T typ
T_{MIN} to T_{MAX}	1.21 ± 7 %	V min/max
REFIN Input Impedance	10	MΩ typ
Reference TC	100	ppm/ °C typ
REFOUT Output Impedance	300	Ω typ
POWER SUPPLIES		
AVDD	4.75/5.25	V min/V max
DVDD	4.75/5.25	V min/V max
IA	5	mA max
IDD	2.5 + 0.33/MHz	mA typ
IA + IDD	40	mA max
Low Power Sleep Mode	0.35	mA max

A.4 AD8130 - High Frequency Differential Receiver Amplifier

Table A.3
Specifications of the AD8130.

Parameter	AD8130	Units
DYNAMIC PERFORMANCE		
-3 dB Bandwidth	270	MHz
$V_{OUT} \leq 0.3 \leq V_{pp}$	200	MHz
$V_{OUT} = 2\ V_{pp}$	± 155	MHz
Bandwidth for 0.1 dB Flatness, $V_{OUT} \leq 0.3$	45	MHz
Slew Rate, $V_{OUT} = 2V_{pp}$	1090	V/μs
NOISE/DISTORTION, Pin VMAG		
Second Harmonic/Third Harmonic	30	mV
$V_{OUT} = 1\ V_{pp}$, 5MHz	-79/-86	dBc
$V_{OUT} = 2\ V_{pp}$, 5MHz	-74/-81	dBc
$V_{OUT} = 1\ V_{pp}$, 10MHz	-74/-80	dBc
$V_{OUT} = 1\ V_{pp}$, 10MHz	-74/-76	dBc
Input Current Noise, f $\geq$ 100 kHz	1	pA/$\sqrt{Hz}$
Differential Gain Error, G = 2	0.13	%
INPUT CHARACTERISTICS,		
Common-Mode Rejection Ratio, V_{CM} = -3 V to +3.5 V	110	dB
$V_{CM} = 1\ V_{pp}$ @ 2 MHz	80 min	dB
$V_{CM} = 1\ V_{pp}$ @ 10 MHz	70	dB
CMRR with $V_{OUT} = 1\ V_{pp}$	83	dB
Differential Resistance	6	MΩ
Common-Mode Resistance	4	MΩ
Differential Capacitance	3	pF
Common-Mode Capacitance	4	pF
OUTPUT PERFORMANCE		
Voltage Swing, R_{LOAD} = 150 Ω/1 kΩ	3.6/4.0	±V
Output Current	40	mA
Output Impedance, In Power-Down Mode	10	pF
POWER SUPPLY		
Operating Voltage Range	2.25 - 12.6	V
Quiescent Supply Current	10.8 typ	mA

REFERENCES

1. Hinton A. J. and Sayers B., "Advanced Instrumentation for Bioimpedance Measurements," *Solartron, Victoria Rd., Farnborough, Hampshire UK,* , 1998.

2. Schmukler R., Bo J., and Davis C., "The measurement of electrical impedance of biologic materials," *Annual International Conference of the IEEE Engineering in Medicine and Biology Society,* Vol. 12, No. 4, 1990.

3. Steendijk P., Mur G., Van Der Velde E. T., and Baan J., "The Four Electrode Resistivity Technique in Anisotropic Media: Theoretical Analysis and Application on Myocardial Tissue in Vivo," *IEEE Transactions on Biomedical Engineering*, Vol. 40, No. 11, 1993.

4. Yang Y., Wang J., Yu G., Niu F., and He P., "Design and preliminary evaluation of a portable device for the measurement of bioimpedance spectroscopy," *Physiol. Meas.*, Vol. 27, pp. 1293-1310, 2006.

5. Palko T., Bialokoz F., and Weglarz J., "Multifrequency Device for Measurement of the Complex Electrical Bio-impedance - Design and Application," *Proceedings RC IEEE-EMBS & BMESI.*, 1995.

6. Min M., Kink A., Land R., Parve T., and Rätsep I., "Modification of Pulse Wave Signals in Electrical Bioimpedance Analyzers for Implantable Medical Devices," *Proceedings, Conference of the IEEE EMBS.*, San Francisco, CA, USA, 2004.

7. Agilent Technologies, "Impedance Measurement Handbook," 2001.

8. Kyle U. G., Bosaeus I., De Lorenzo A. D., et al, "Bioelectrical impedance analysis-part I: review of principles and methods," *Clinical Nutrition*, Vol. 23, pp. 1226-1243, 2004.

9. Ulgen Y., and Sezdi M., "Hemotocrit Dependence of the Cole-Cole Parameters of Human Blood," *IEEE 2nd International Biomedical Engineering Days*, 1998.

10. M. Sezdi, M. Bayık and Y. Ulgen, "Storage effects on the Cole-Cole parameters of erythrocyte suspensions," *Appl. Physiol.*, Vol. 27, pp. 623-635, 2006.

11. Webster, J.G., *Electrical Impedance Tomography,* Adam Hilger, Bristol and New York, 1990.

12. Leigh C. Ward, Essex T., and Cornish B. H., "Determination of Cole parameters in multiple frequency bioelectrical impedance analysis using only the measurement of impedances," *Physiol. Meas.*, Vol. 27, pp. 839-850, 2006.

13. Yang Y., and Wang J., "New Tetrapolar Method for Complex Bioimpedance Measurement: Theoretical Analysis and Circuit Realization," *Proceedings, IEEE Engineering in Medicine and Biology 27th Annual Conference*, Shanghai, China, 2005.

14. Murphy E., Slattery C., "All About Direct Direct Digital Synthesis," *Analog Dialogue*, Vol. 38, 2004.

15. "AD9835: 50MHz CMOS Complete DDS," Datasheet.

16. "CA3280: Dual 9MHz Operational Transconductance Amplifier," Datasheet.

17. "AD8129: Low-cost 270MHz Differential Receiver Amplifiers," Datasheet.

18. "AD8302: LF-2.7GHz RF/IF Gaşn and Phase Detector," Datasheet.

19. Bao J.Z., Davis C. C. and Schmukler R. E:, "Impedance system spectroscopy of human erythrocytes calibration and nonlinear modeling," *J. IEEE Transactions on Biomedical Engineering*, Vol. 40, pp. 364-378, 1993.

20. Tsai J. Z., Will J. A., Van Stelle S. H., Cao H., Tungjitkusolmun S., Choy Y. B., Haemmerich D., Vorperian V. R., and Webster J. G., "Error Analysis of Tissue Resistivity Measurement," *J. IEEE Transactions on Biomedical Engineering*, Vol. 49, No. 5, 2002.